Whistler wave radiation from a pulsed loop antenna located in a cylindrical duct with enhanced plasma density

Alexander V. Kudrin, Natalya M. Shkokova, Orsolya E. Ferencz, and Tatyana M. Zaboronkova

Citation: Physics of Plasmas (1994-present) **21**, 112115 (2014); doi: 10.1063/1.4901949
View online: http://dx.doi.org/10.1063/1.4901949
View Table of Contents: http://scitation.aip.org/content/aip/journal/pop/21/11?ver=pdfcov
Published by the AIP Publishing

Whistler wave radiation from a pulsed loop antenna located in a cylindrical duct with enhanced plasma density

Alexander V. Kudrin,[1] Natalya M. Shkokova,[1] Orsolya E. Ferencz,[2] and Tatyana M. Zaboronkova[1,3]
[1]*Department of Radiophysics, University of Nizhny Novgorod, 23 Gagarin Ave., Nizhny Novgorod 603950, Russia*
[2]*MTA Research Centre for Astronomy and Earth Sciences, Csatkai E. u. 6–8, Sopron H-9400, Hungary*
[3]*Department of Nuclear Physics, R. E. Alekseev State Technical University of Nizhny Novgorod, 24 Minin St., Nizhny Novgorod 603950, Russia*

(Received 3 August 2014; accepted 5 November 2014; published online 21 November 2014)

Pulsed radiation from a loop antenna located in a cylindrical duct with enhanced plasma density is studied. The radiated energy and its distribution over the spatial and frequency spectra of the excited waves are derived and analyzed as functions of the antenna and duct parameters. Numerical results referring to the case where the frequency spectrum of the antenna current is concentrated in the whistler range are reported. It is shown that under ionospheric conditions, the presence of an artificial duct with enhanced density can lead to a significant increase in the energy radiated from a pulsed loop antenna compared with the case where the same source is immersed in the surrounding uniform magnetoplasma. The results obtained can be useful in planning active ionospheric experiments with pulsed electromagnetic sources operated in the presence of artificial field-aligned plasma density irregularities that are capable of guiding whistler waves. © *2014 AIP Publishing LLC*.
[http://dx.doi.org/10.1063/1.4901949]

I. INTRODUCTION

Electromagnetic radiation from monochromatic sources embedded in homogeneous and inhomogeneous magnetized plasmas has been studied in many publications (see, e.g., works[1–24] and references therein). A great deal of attention has particularly been devoted to whistler wave excitation in laboratory and space plasmas containing magnetic-field-aligned density irregularities.[10–22] Such irregularities, commonly known as density ducts, can exist in the Earth's magnetosphere, in which they ensure guidance of whistler-mode waves naturally occurring under space plasma conditions.[25] Of no less interest are artificial density ducts that can arise due to various nonlinear effects near electromagnetic sources in laboratory and space plasmas. A number of important features of whistler wave radiation from monochromatic sources in the presence of density ducts have been documented in Refs. 10–20. In particular, it has been demonstrated that under certain conditions, the presence of a duct can significantly improve the antenna coupling into whistler-mode waves.[16–20] For example, the radiation resistance of a loop antenna located in a duct with enhanced density can be notably greater than that in the case where such a source is immersed in a uniform background plasma of lower density.[14,16,18] This circumstance can evidently be used for many promising applications, some of which are discussed in Refs. 16 and 19.

Over the past two decades, there has been shown a substantial degree of interest in the excitation of nonmonochromatic waves propagating in the whistler mode in a magnetoplasma.[26–33] This interest has been motivated by the importance of transient phenomena for propagation of whistler-mode waves through the magnetosphere and the ionosphere, as well as for plasma diagnostics using pulsed signals launched from antennas on spacecraft in the whistler range. However, much previous theoretical work on the subject is mainly focused on studying the fields and radiation characteristics of nonmonochromatic sources in a homogeneous magnetoplasma. At the same time, little is known about the radiation characteristics of pulsed sources of even simple geometry in the presence of density ducts.

It is the purpose of the present article to study the energy radiation characteristics of a pulsed loop antenna located in an enhanced-density duct that is surrounded by a uniform cold magnetoplasma such as exists in the Earth's ionosphere. To solve the formulated problem, we will use a rigorous full-wave approach throughout the article and apply this analysis to the case where the frequency spectrum of the antenna current is concentrated in the whistler range. Such an analysis is topical in view of the fact that corresponding conditions are typical of many modeling laboratory[13,17] and active ionospheric[34] experiments. Moreover, determination of the radiation characteristics of a pulsed loop antenna in the presence of an enhanced-density duct seems crucial to understanding the influence of such a duct on the antenna radiation characteristics as compared to the case of monochromatic excitation. In order to elucidate the physical aspects of the formulated problem more clearly, we confine ourselves to the case where the loop axis is aligned with the duct axis, which is parallel to an external dc magnetic field. Note that such orientation is very suitable for many applications, and has been used in numerous laboratory experiments aimed at modeling the loop antenna operation in a magnetoplasma containing a density duct.[10–13,17] We will also compare the efficiency of

whistler wave excitation by a pulsed loop antenna in the presence of a density enhancement with the corresponding results referring to the case where such an antenna is immersed in a homogeneous magnetoplasma, which has been analyzed in our recent work.[33]

Our article is organized as follows. In Sec. II, we formulate the studied problem and describe our theoretical approach. In Sec. III, the source-excited field in the presence of a cylindrical density duct is obtained. In Sec. IV, a rigorous representation for the total energy radiated from a pulsed loop antenna is derived. Then, in Sec. V, we apply the derived representation for analysis of the radiation characteristics of such an antenna and calculate numerically the antenna radiated energy and its distribution over the spatial and frequency spectra of the excited waves under conditions typical of active ionospheric experiments with loop antennas. Section VI states our conclusions and suggestions for future work.

II. FORMULATION OF THE PROBLEM AND BASIC EQUATIONS

Consider a cylindrical density duct of radius a. The duct is aligned with the z axis of a cylindrical coordinate system (ρ, ϕ, z). Parallel to this axis is a uniform dc magnetic field $\mathbf{B}_0 = B_0\hat{\mathbf{z}}$. The duct is surrounded by a uniform background magnetoplasma. The electromagnetic field is excited by a circular loop antenna placed coaxially in the duct.

Assuming that the medium inside and outside the duct is a cold collisionless magnetoplasma, we can write its dielectric tensor in the form

$$\boldsymbol{\varepsilon} = \epsilon_0 \begin{pmatrix} \varepsilon & -ig & 0 \\ ig & \varepsilon & 0 \\ 0 & 0 & \eta \end{pmatrix}, \tag{1}$$

where ϵ_0 is the permittivity of free space. For a monochromatic signal with a time dependence of $\exp(i\omega t)$, the tensor elements ε, g, and η in the case of a two-component magnetoplasma are written as[19,35]

$$\begin{aligned} \varepsilon &= \frac{(\omega^2 - \omega_{\mathrm{LH}}^2)(\omega^2 - \omega_{\mathrm{UH}}^2)}{(\omega^2 - \omega_c^2)(\omega^2 - \Omega_c^2)}, \\ g &= \frac{\omega_p^2\, \omega_c\, \omega}{(\omega^2 - \omega_c^2)(\omega^2 - \Omega_c^2)}, \\ \eta &= 1 - \frac{\omega_p^2}{\omega^2}, \end{aligned} \tag{2}$$

where ω_p is the electron plasma frequency, Ω_c and ω_c are the ion and electron cyclotron frequencies, and ω_{LH} and ω_{UH} are the lower and upper hybrid frequencies, respectively. Recall that the latter two frequencies can be written, to a good approximation, as[19]

$$\omega_{\mathrm{UH}} = \left(\omega_p^2 + \omega_c^2\right)^{1/2}, \quad \omega_{\mathrm{LH}} = \omega_c \left(\frac{\Omega_p^2 + \Omega_c^2}{\omega_p^2 + \omega_c^2}\right)^{1/2}, \tag{3}$$

where Ω_p is the ion plasma frequency. In this work, we confine ourselves to consideration of the case where

$$\Omega_c \ll \omega_{\mathrm{LH}} \ll \omega_c \ll \omega_p < \omega_{\mathrm{UH}}, \tag{4}$$

which is typical of a magnetoplasma modeled upon the Earth's ionosphere. Under such conditions, the lower hybrid frequency is reduced to the form $\omega_{\mathrm{LH}} = (\Omega_c\omega_c)^{1/2}$ and thus becomes independent of the plasma (electron number) density.

The plasma density is equal to $\tilde{N}$ inside the duct, and to N_a in the ambient uniform plasma surrounding the duct. Accordingly, the elements of tensor (1), which are functions of the plasma density, are different in the inner and outer regions of the duct. In what follows, the tensor elements and the electron plasma frequency will be denoted as $\tilde{\varepsilon}$, $\tilde{g}$, $\tilde{\eta}$, and $\tilde{\omega}_p$ for $\rho < a$ and as ε_a, g_a, η_a, and ω_{pa} for $\rho > a$. We will be considering the case of a sharp-walled uniform duct, for which $\tilde{N} = \text{const}$. It will be explained below that this assumption does not lead to any loss of generality when analyzing the basic features of operation of a pulsed loop antenna in the presence of the duct.

The density of the electric current in the antenna, which excites the electromagnetic radiation, is specified in the form

$$\mathbf{J}(\mathbf{r}, t) = \hat{\boldsymbol{\phi}} I_0 \delta(\rho - b)\delta(z)\chi(t), \tag{5}$$

where I_0 is the amplitude of total current, b is the antenna radius $(b < a)$, δ is a Dirac function, and $\chi(t)$ is a dimensionless function which describes the current behavior in time. The function $\chi(t)$ has the maximum value equal to unity and differs from zero in the time interval $0 < t < \tau$. Here, τ is the current pulse duration, which can be either finite or infinite.

In this article, we will focus on studying the radiation from a loop antenna placed in an enhanced-density duct, for which $\tilde{N} > N_a$. This is motivated by the fact that the radiation resistance of a time-harmonic loop antenna located in such a duct is known to increase with increasing ratio $\tilde{N}/N_a$ if the frequency of the antenna current lies in the whistler range.[19] Therefore, it seems important to analyze the influence of the duct on the radiation efficiency of the same source in a pulsed regime. On the other hand, it is also expedient to compare the radiation characteristics of the pulsed loop antenna located in such a duct with those in the case where the corresponding source is immersed in a homogeneous unbounded magnetoplasma.[33] To this end, we choose the temporal behavior of the antenna current in the form coinciding with that in Ref. 33, i.e., take a pulse whose filling comprises a few half-periods of a monochromatic oscillation

$$\chi(t) = [H(t) - H(t - \tau)]\sin(\omega_0 t). \tag{6}$$

Here, $H(t)$ is a Heaviside function, ω_0 is a certain frequency corresponding to a given period $T = 2\pi/\omega_0$, and the pulse duration $\tau = nT/2 = \pi n/\omega_0$, where $n = 1, 2, \ldots$. In addition, we will also examine the case of a single current pulse without modulation

$$\chi(t) = \frac{t}{t_0}\exp\left(-\frac{t - t_0}{t_0}\right). \tag{7}$$

In what follows, we will take the current pulse (7) for $t_0 = T/4 \equiv \pi/2\omega_0$. In this case, such a pulse is similar in shape to the pulse described by Eq. (6) for $n=1$, which makes it reasonable to compare the radiation characteristics of the two sources.

Our main task is to study the efficiency of excitation of electromagnetic waves which are emitted from the current source (5) located in a density duct. To proceed in this way, we should analyze the radiated energy of this source in the presence of the duct. As is known, the total energy W radiated from an electric current $\mathbf{J}(\mathbf{r}, t)$ with duration τ can be obtained as

$$W = -\int_0^\tau dt \int_V \mathbf{J}(\mathbf{r},t)\cdot\mathbf{E}(\mathbf{r},t)d\mathbf{r}, \tag{8}$$

where integration with respect to the spatial coordinates is performed over the volume V occupied by the antenna current, and $\mathbf{E}(\mathbf{r}, t)$ is the total electric field excited by the antenna. It is worth mentioning that this field comprises not only the nonradiative part, which is predominant near the source, but also the radiative part responsible for the outgoing energy transport. To evaluate W, we need to express $\mathbf{E}(\mathbf{r}, t)$ in terms of the antenna current.

III. FIELD EXPANSION IN THE PRESENCE OF A DENSITY DUCT

The field excited by a pulsed source can be represented using the Laplace transform technique

$$\begin{bmatrix}\mathbf{E}(\mathbf{r},t)\\ \mathbf{B}(\mathbf{r},t)\end{bmatrix} = \frac{1}{2\pi}\int_{-i\sigma-\infty}^{-i\sigma+\infty}\begin{bmatrix}\mathbf{E}(\mathbf{r},\omega)\\ \mathbf{B}(\mathbf{r},\omega)\end{bmatrix}\exp(i\omega t)d\omega. \tag{9}$$

Here, σ is a real-valued positive constant and ω is a complex-valued quantity such that $\omega = \mathrm{Re}\omega - i\sigma$. A similar formula can be written to relate the current density $\mathbf{J}(\mathbf{r}, t)$ and its Laplace transform $\mathbf{J}(\mathbf{r}, \omega)$.

To represent the Laplace-transformed fields $\mathbf{E}(\mathbf{r}, \omega)$ and $\mathbf{B}(\mathbf{r}, \omega)$ in terms of $\mathbf{J}(\mathbf{r}, \omega)$, we apply the formulation based on the eigenfunction expansion of the source-excited field.[17–20] According to this approach, the quantities $\mathbf{E}(\mathbf{r}, \omega)$ and $\mathbf{B}(\mathbf{r}, \omega)$, which are independent of the azimuthal coordinate ϕ because of the symmetry of the problem, are expanded in terms of the vector eigenfunctions of the discrete and continuous spectrum

$$\begin{aligned}\begin{bmatrix}\mathbf{E}(\mathbf{r},\omega)\\ \mathbf{B}(\mathbf{r},\omega)\end{bmatrix} &= \sum_n a_{s,n}(\omega)\begin{bmatrix}\mathbf{E}_{s,n}(\rho,\omega)\\ \mathbf{B}_{s,n}(\rho,\omega)\end{bmatrix}\\ &\quad\times\exp[-ih_{s,n}(\omega)z]\\ &\quad+\sum_\alpha\int_0^\infty a_{s,\alpha}(k_\perp,\omega)\begin{bmatrix}\mathbf{E}_{s,\alpha}(\rho,k_\perp,\omega)\\ \mathbf{B}_{s,\alpha}(\rho,k_\perp,\omega)\end{bmatrix}\\ &\quad\times\exp[-ih_{s,\alpha}(k_\perp,\omega)z]dk_\perp.\end{aligned} \tag{10}$$

Here, $h_{s,n}$ is the propagation constant of an eigenmode (discrete-spectrum wave) with the radial index n ($n=1,2,\ldots$), $\mathbf{E}_{s,n}(\rho, \omega)$ and $\mathbf{B}_{s,n}(\rho, \omega)$ are the vector functions describing the radial distribution of the field of this eigenmode, $a_{s,n}(\omega)$ is its excitation coefficient, $k_\perp$ is the transverse (with respect to $\mathbf{B}_0$) wave number in the outer region, $h_{s,\alpha}(k_\perp, \omega)$ is the longitudinal wave number for two characteristic waves of a uniform background magnetoplasma, which are denoted by the subscripts $\alpha=1$ and $\alpha=2$, $\mathbf{E}_{s,\alpha}(\rho, k_\perp, \omega)$ and $\mathbf{B}_{s,\alpha}(\rho, k_\perp, \omega)$ are the vector functions describing the radial distribution of the field of a continuous-spectrum wave that corresponds to the transverse wave number $k_\perp$ and the subscript α, $a_{s,\alpha}(k_\perp, \omega)$ is the excitation coefficient of the respective wave, and the subscript s denotes the wave propagation direction ($s=-$ and $s=+$ designate waves propagating in the negative and positive directions of the z axis, respectively). The propagation constants $h_{s,n}$ obey the relationships $h_{+,n} \equiv h_n = -h_{-,n}$, where $\mathrm{Im}\, h_n < 0$. The quantities $h_{s,\alpha}$ satisfy the analogous relationships $h_{+,\alpha} \equiv h_\alpha = -h_{-,\alpha}$, where $h_\alpha^2(k_\perp, \omega)$ is given by the expression

$$\begin{aligned}h_\alpha^2(k_\perp,\omega) &= k_0^2\varepsilon_a - \frac{1}{2}\left(1+\frac{\varepsilon_a}{\eta_a}\right)k_\perp^2 + \gamma_\alpha\\ &\quad\times\left[\frac{1}{4}k_\perp^4\left(1-\frac{\varepsilon_a}{\eta_a}\right)^2 - k_0^2k_\perp^2\frac{g_a^2}{\eta_a} + k_0^4g_a^2\right]^{1/2}.\end{aligned} \tag{11}$$

Here, $k_0 = \omega/c$ (c is the speed of light in free space), $\gamma_1 = -\gamma_2 = 1$, and the tensor elements ε_a, g_a, and η_a are taken at the complex frequency ω and correspond to the parameters of the plasma surrounding the duct. The square root in Eq. (11) is defined so as to have the positive real part, whereas the function h_α satisfies the condition $\mathrm{Im}\, h_\alpha < 0$.

Since the procedure of obtaining the vector wave functions in expansion (10) is thoroughly described in the literature,[17–20] we dwell only briefly on the main steps of the derivation of these functions. We start from the continuous-spectrum waves. It can be shown from Maxwell's equations that the vector functions $\mathbf{E}_{s,\alpha}(\rho, k_\perp, \omega)$ and $\mathbf{B}_{s,\alpha}(\rho, k_\perp, \omega)$ can be expressed in terms of their azimuthal components $E_{\phi;s,\alpha}(\rho, k_\perp, \omega)$ and $B_{\phi;s,\alpha}(\rho, k_\perp, \omega)$ which satisfy the system of equations[19]

$$\begin{aligned}&\frac{\partial}{\partial\rho}\left[\frac{1}{\rho}\frac{\partial}{\partial\rho}(\rho E_{\phi;s,\alpha})\right] - \left[h_{s,\alpha}^2 + k_0^2\left(\frac{g^2}{\varepsilon}-\varepsilon\right)\right]E_{\phi;s,\alpha}\\ &\quad + ik_0\frac{g}{\varepsilon}h_{s,\alpha}cB_{\phi;s,\alpha} = 0,\end{aligned} \tag{12}$$

$$\begin{aligned}&\frac{\partial}{\partial\rho}\left[\frac{1}{\rho}\frac{\partial}{\partial\rho}(\rho B_{\phi;s,\alpha})\right] - \frac{\eta}{\varepsilon}\left(h_{s,\alpha}^2 - k_0^2\varepsilon\right)B_{\phi;s,\alpha}\\ &\quad - ik_0\frac{g\eta}{\varepsilon}h_{s,\alpha}c^{-1}E_{\phi;s,\alpha} = 0,\end{aligned} \tag{13}$$

into which the tensor elements corresponding to the outer or inner region of the duct should be substituted when finding the solutions for $\rho > a$ and $\rho < a$, respectively. The solutions should ensure the boundedness of the quantities $\rho^{1/2}|\mathbf{E}_{s,\alpha}(\rho, k_\perp, \omega)|$ and $\rho^{1/2}|\mathbf{B}_{s,\alpha}(\rho, k_\perp, \omega)|$ at $\rho \to \infty$, whence it follows that the field components of the continuous-spectrum waves in the outer region ($\rho > a$) are written as[19]

$$E_{\phi;s,\alpha}(\rho,k_\perp,\omega)=i\left[\sum_{k=1}^{2}C_{s,\alpha}^{(k)}H_1^{(k)}(k_\perp\rho)+D_{s,\alpha}H_1^{(2)}(k_{\perp\alpha}\rho)\right], \tag{14}$$

$$B_{\phi;s,\alpha}(\rho,k_\perp,\omega)=-c^{-1}\left[\sum_{k=1}^{2}C_{s,\alpha}^{(k)}n_{s,\alpha}^{(1)}H_1^{(k)}(k_\perp\rho)+D_{s,\alpha}n_{s,\alpha}^{(2)}H_1^{(2)}(k_{\perp\alpha}\rho)\right]. \tag{15}$$

Here, $H_1^{(1,2)}$ are Hankel functions of the first and second kinds, $C_{s,\alpha}^{(k)}$ and $D_{s,\alpha}$ are coefficients to be determined, $k=1$, 2, and

$$n_{s,\alpha}^{(k)}=-\varepsilon_a\left[\left(k_{\perp\alpha}^{(k)}\right)^2+h_\alpha^2+k_0^2\left(\frac{g_a^2}{\varepsilon_a}-\varepsilon_a\right)\right](k_0h_{s,\alpha}g_a)^{-1},$$
$$k_{\perp\alpha}^{(1)}=k_\perp,\quad k_{\perp\alpha}^{(2)}=k_{\perp\alpha}=\left[k_0^2\varepsilon_a-h_\alpha^2-k_0^2\frac{g_a}{\varepsilon_a}\left(g_a-\frac{\eta_a h_{s,\alpha}}{k_0n_{s,\alpha}^{(1)}}\right)\right]^{1/2}, \tag{16}$$

where it is assumed that the quantity $k_{\perp\alpha}$, which can be called the auxiliary transverse wave number in the outer region, satisfies the inequality $\mathrm{Im}\,k_{\perp\alpha}<0$. With such a choice of $k_{\perp\alpha}$, the presence of the second-kind Hankel functions $H_1^{(2)}(k_{\perp\alpha}\rho)$ in Eqs. (14) and (15) does not contradict the boundedness condition for the continuous-spectrum waves at $\rho\to\infty$. Note that in a lossless medium, the auxiliary transverse wave number may be purely real for some values of $k_\perp$. In such a case, one should introduce infinitesimally small losses, choose the proper branch of $k_{\perp\alpha}$ according to the adopted condition for $\mathrm{Im}\,k_{\perp\alpha}$, and then put the losses equal to zero.

The solution for the field in the inner region ($\rho<a$) is written as

$$E_{\phi;s,\alpha}(\rho,k_\perp,\omega)=i\sum_{k=1}^{2}A_{s,\alpha}^{(k)}J_1(\tilde{k}_{\perp\alpha}^{(k)}\rho), \tag{17}$$

$$B_{\phi;s,\alpha}(\rho,k_\perp,\omega)=-c^{-1}\sum_{k=1}^{2}A_{s,\alpha}^{(k)}\tilde{n}_{s,\alpha}^{(k)}J_1(\tilde{k}_{\perp\alpha}^{(k)}\rho), \tag{18}$$

where J_1 is a Bessel function of the first kind, $A_{s,\alpha}^{(k)}$ are coefficients to be determined, and

$$\tilde{n}_{s,\alpha}^{(k)}=-\tilde{\varepsilon}\left[\left(\tilde{k}_{\perp\alpha}^{(k)}\right)^2+h_\alpha^2+k_0^2\left(\frac{\tilde{g}^2}{\tilde{\varepsilon}}-\tilde{\varepsilon}\right)\right](k_0h_{s,\alpha}\tilde{g})^{-1},$$
$$\tilde{k}_{\perp\alpha}^{(k)}=\frac{1}{\sqrt{2}}\left\{k_0^2\left(\tilde{\varepsilon}-\frac{\tilde{g}^2}{\tilde{\varepsilon}}+\tilde{\eta}\right)-\left(\frac{\tilde{\eta}}{\tilde{\varepsilon}}+1\right)h_\alpha^2-\left(\frac{\tilde{\eta}}{\tilde{\varepsilon}}-1\right)\right.$$
$$\left.\times(-1)^k\left\{\left[h_\alpha^2-k_0^2\mathcal{P}_b^2(\tilde{N})\right]\left[h_\alpha^2-k_0^2\mathcal{P}_c^2(\tilde{N})\right]\right\}^{1/2}\right\}^{1/2}. \tag{19}$$

The quantities $\mathcal{P}_b$ and $\mathcal{P}_c$ for a homogeneous plasma of density N are determined by the expression

$$\mathcal{P}_{b,c}(N)=\left\{\varepsilon-(\eta+\varepsilon)\frac{g^2}{(\eta-\varepsilon)^2}+\frac{2\chi_{b,c}}{(\eta-\varepsilon)^2}\right.$$
$$\left.\times\left\{\varepsilon g^2\eta\left[g^2-(\eta-\varepsilon)^2\right]\right\}^{1/2}\right\}^{1/2}, \tag{20}$$

where $\chi_b=-\chi_c=-1$. The tensor elements on the right-hand side of (20) are taken for the indicated plasma density N.

To find the unknown coefficients $A_{s,\alpha}^{(1,2)}$, $C_{s,\alpha}^{(1,2)}$, and $D_{s,\alpha}$ in Eqs. (14), (15), (17), and (18), we should satisfy the continuity conditions for the tangential field components at $\rho=a$, which yields the system of four linear equations. This system can be represented in matrix form

$$\boldsymbol{S}\cdot\mathbf{G}=C_{s,\alpha}^{(1)}\mathbf{F}, \tag{21}$$

where the elements of the column vector $\mathbf{G}$ are given by the expressions $G_{1,2}=A_{s,\alpha}^{(1,2)}$, $G_3=C_{s,\alpha}^{(2)}$, and $G_4=D_{s,\alpha}$. The elements of the matrix $\boldsymbol{S}$ and the components of the column vector $\mathbf{F}$ are expressed in an evident manner via the tangential fields on both sides of the interface $\rho=a$ and are not written here for brevity. Since Eq. (21) gives four linear relationships for five coefficients $A_{s,\alpha}^{(1,2)}$, $C_{s,\alpha}^{(1,2)}$, and $D_{s,\alpha}$, one of them can be taken arbitrary. This circumstance reflects the fact that the mode fields are defined up to an arbitrary factor independent of the spatial coordinates. It is most convenient to put $C_{s,\alpha}^{(1)}=\det||\boldsymbol{S}||$ and then determine the remaining coefficients from Eq. (21). The advantage of such a choice is related to the fact that the quantities $k_\perp=k_{\perp n}$ which are zeros of the coefficient $C_{s,\alpha}^{(1)}$ and satisfy the condition $\mathrm{Im}\,k_{\perp n}<0$ determine the transversely localized eigenmodes (discrete-spectrum waves) guided by the duct in some frequency ranges. Substituting the quantities $k_\perp=k_{\perp n}$ into $\mathbf{E}_{s,\alpha}(\rho,k_\perp,\omega)$, $\mathbf{B}_{s,\alpha}(\rho,k_\perp,\omega)$, and $h_\alpha(k_\perp,\omega)$, one can obtain the fields $\mathbf{E}_{s,n}(\rho,\omega)$ and $\mathbf{B}_{s,n}(\rho,\omega)$ and the propagation constants $h_n(\omega)$ of the corresponding eigenmodes.[15,19] Note that the eigenmode fields comprise the contributions with two different transverse wave numbers both inside and outside the duct ($\tilde{k}_{\perp\alpha}^{(1)}$ and $\tilde{k}_{\perp\alpha}^{(2)}$ for $\rho<a$, and $k_{\perp n}$ and $k_{\perp\alpha}$ for $\rho>a$), which correspond to the same propagation constant h_n. This fact is stipulated by the gyrotropic properties of a magnetoplasma containing the duct.

Once the discrete- and continuous-spectrum waves are found, their excitation coefficients can be determined using the standard technique developed for open waveguides[19]

$$\begin{bmatrix}a_{\pm,n}(\omega)\\ a_{\pm,\alpha}(k_\perp,\omega)\end{bmatrix}=\begin{bmatrix}N_n^{-1}(\omega)\\ N_\alpha^{-1}(k_\perp,\omega)\end{bmatrix}\int_V\mathbf{J}(\mathbf{r},\omega)\cdot\begin{bmatrix}\mathbf{E}_{\mp,n}^{(\mathrm{T})}(\mathbf{r},\omega)\\ \mathbf{E}_{\mp,\alpha}^{(\mathrm{T})}(\mathbf{r},k_\perp,\omega)\end{bmatrix}d\mathbf{r}. \tag{22}$$

Here, integration is performed over the region V occupied by the current $\mathbf{J}$, the superscript (T) denotes fields taken in a medium described by the transposed dielectric tensor $\boldsymbol{\varepsilon}^{\mathrm{T}}$, $\mathbf{E}_{s,n}(\mathbf{r},\omega)=\mathbf{E}_{s,n}(\rho,\omega)\exp[-ih_{s,n}(\omega)z]$, $\mathbf{E}_{s,\alpha}(\mathbf{r},k_\perp,\omega)=\mathbf{E}_{s,\alpha}(\rho,k_\perp,\omega)\exp[-ih_{s,\alpha}(k_\perp,\omega)z]$, and the normalization quantities $N_n(\omega)$ and $N_\alpha(k_\perp,\omega)$ for modes are given by

$$N_n(\omega) = \frac{2\pi}{\mu_0}\int_0^\infty \left[\mathbf{E}_{+,n}(\rho,\omega)\times\mathbf{B}^{(\mathrm{T})}_{-,n}(\rho,\omega) - \mathbf{E}^{(\mathrm{T})}_{-,n}(\rho,\omega)\times\mathbf{B}_{+,n}(\rho,\omega)\right]\cdot\hat{\mathbf{z}}\,\rho\,d\rho,$$
$$N_\alpha(k_\perp,\omega) = -\frac{16\pi}{Z_0 k_0}\left(\frac{dh_\alpha(k_\perp,\omega)}{dk_\perp}\right)^{-1}\left[1+\eta_a^{-1}\left(n^{(1)}_{+,\alpha}\right)^2\right]C^{(1)}_{+,\alpha}C^{(2)}_{+,\alpha}, \tag{23}$$

where μ_0 is the permeability of free space and $Z_0 = (\mu_0/\epsilon_0)^{1/2}$ is the free-space impedance. The obtained modal representation with the coefficients of Eq. (22) yields the rigorous solution for the total Laplace-transformed field at the complex frequency ω and allows one to immediately determine the individual contributions of the guided (discrete-spectrum) waves and of the remaining part of the field, represented by integrals over unguided (continuous-spectrum) waves, to the source-excited field.

IV. ENERGY RADIATED

The total energy W radiated from a loop antenna with current (5) is determined only by the azimuthal electric-field component. With allowance for the results of the preceding section, the Laplace transform $E_\phi(\mathbf{r},\omega)$ of this component is given by the expression

$$E_\phi(\mathbf{r},\omega) = \sum_n a_{s,n}(\omega)E_{\phi;s,n}(\rho,\omega)\exp[-ih_{s,n}(\omega)z] + \sum_\alpha\int_0^\infty a_{s,\alpha}(k_\perp,\omega)E_{\phi;s,\alpha}(\rho,k_\perp,\omega) \times \exp[-ih_{s,\alpha}(k_\perp,\omega)z]dk_\perp. \tag{24}$$

According to Eq. (22), the excitation coefficients in Eq. (24) are written as

$$a_{\pm,n}(\omega) = 2\pi b I_0\chi(\omega)N_n^{-1}(\omega)E^{(\mathrm{T})}_{\phi;\mp,n}(b,\omega),$$
$$a_{\pm,\alpha}(k_\perp,\omega) = 2\pi b I_0\,\chi(\omega)\,N_\alpha^{-1}(k_\perp,\omega)E^{(\mathrm{T})}_{\phi;\mp,\alpha}(b,k_\perp,\omega), \tag{25}$$

where $\chi(\omega)$ is the Laplace transform of the function $\chi(t)$ describing the time behavior of the source current.

Substituting the inverse Laplace transform of the quantity $E_\phi(\mathbf{r},\omega)$ into Eq. (8) and performing integration with respect to the spatial coordinates and time, we obtain

$$W = -I_0 b\int_{-i\sigma-\infty}^{-i\sigma+\infty} d\omega\,\chi(-\omega)E_\phi(\mathbf{r},\omega)|_{\rho=b,\,z=0}\,. \tag{26}$$

The integration path in (26) is symmetric about the imaginary ω axis. Hence, any two frequencies ω' and ω'' which belong to the path of integration over the frequency and are located on this path symmetrically about the imaginary ω axis are related as $\omega'^* = -\omega''$, where the asterisk stands for complex conjugate. Allowing for this fact, we pass to integration over the right-hand part of this path, for which Re $\omega > 0$, and make the limiting transition $\sigma \to 0$. As a result, we arrive at the expression

$$W = I_0^2\int_0^\infty w(\omega)d\omega = I_0^2\int_0^\infty\left[\sum_n w_n(\omega) + \sum_\alpha\int_{Q_\alpha} w_\alpha(q,\omega)dq\right]d\omega, \tag{27}$$

where

$$w_n(\omega) = -4\pi b^2\mathrm{Re}\,[F(\omega)N_n^{-1}(\omega)E^{(\mathrm{T})}_{\phi;-s,n}(b,\omega)E_{\phi;s,n}(b,\omega)], \tag{28}$$

$$w_\alpha(q,\omega) = -4\pi k_0 b^2\mathrm{Re}\,[F(\omega)N_\alpha^{-1}(k_0 q,\omega) \times E^{(\mathrm{T})}_{\phi;-s,\alpha}(b,k_0 q,\omega)E_{\phi;s,\alpha}(b,k_0 q,\omega)]. \tag{29}$$

Here, integration with respect to ω is performed over the positive real frequency semi-axis, $F(\omega) = \chi(\omega)\chi(-\omega)$, $q = k_\perp/k_0$, and the symbol Q_α denotes the regions in the first quadrant of the (ω, q) plane (with $\omega > 0$ and $q > 0$), for which the functions h_α are purely real. Note that we have passed to using the dimensionless transverse wave number q instead of $k_\perp$ in Eq. (27). The allowed regions Q_1 and Q_2 of integration in the (ω, q) plane for evaluating W coincide with those discussed in Ref. 33. It is worth also mentioning that the results yielded by Eqs. (28) and (29) are independent of s due to the symmetry properties of the quantities in these formulas.

We emphasize that only the propagated eigenmodes with purely real propagation constants $h_{s,n}$ and the continuous-spectrum waves corresponding to the above-described integration regions Q_α make nonzero contributions to the radiated energy W. Other waves do not transport energy away from the source and, hence, do not contribute to the radiation from the antenna. Thus, it is evident that the quantities w_n and w_α represent the partial contributions of the propagated eigenmodes and the continuous-spectrum waves, respectively, to the antenna radiation at a fixed frequency, i.e., describe the distribution of the radiated energy over the spatial spectrum of the excited waves. In turn, the function $w(\omega)$ characterizes the distribution of the radiated energy over the frequency spectrum.

The function $F(\omega)$ in cases (6) and (7) is represented as

$$F(\omega) = \left\{\frac{\sin[(\omega-\omega_0)\tau/2]}{\omega-\omega_0} - (-1)^n\frac{\sin[(\omega+\omega_0)\tau/2]}{\omega+\omega_0}\right\}^2 \tag{30}$$

and

$$F(\omega) = (et_0)^2/[1+(\omega t_0)^2]^2, \tag{31}$$

respectively. To avoid misunderstanding, we note that for the source with time dependence (7), the condition $\sigma < t_0^{-1}$

is required in Eq. (26). For $\sigma \to 0$, this condition, which is necessary for the existence of the function $F(\omega)$ defined by Eq. (31), is ensured automatically. Bearing this in mind, it is possible to check that no singularities of the integrands in Eq. (26) are intercepted in the derivation of Eq. (26) when passing to the limit $\sigma \to 0$.

V. NUMERICAL RESULTS FOR THE RADIATION CHARACTERISTICS

The radiated energy W was evaluated numerically for plasma parameters typical of the Earth's ionosphere: the ambient plasma density $N_a = 10^6\,\mathrm{cm}^{-3}$ and the external static magnetic field $B_0 = 0.5\,\mathrm{G}$. With these values, the electron plasma frequency outside the duct and the electron cyclotron frequency were equal to $\omega_{pa} = 5.6 \times 10^7\,\mathrm{s}^{-1}$ and $\omega_c = 8.8 \times 10^6\,\mathrm{s}^{-1}$, respectively. Since the model of a two-component magnetoplasma is employed in this work to describe the properties of the ionospheric plasma, which is actually multi-component, the quantity Ω_c in Eqs. (2) and (3) has the meaning of the effective ion cyclotron frequency. This quantity was chosen equal to $\Omega_c = 200\ \mathrm{s}^{-1}$, in which case the lower-hybrid frequency $\omega_{\mathrm{LH}} = 4.2 \times 10^4\,\mathrm{s}^{-1}$. We assumed that the antenna radius $b = 2.5\,\mathrm{m}$, the duct radius $a = 5\,\mathrm{m}$, and the plasma density $\tilde{N}$ inside the duct (normalized to N_a) varies in the range $10 < \tilde{N}/N_a < 30$. The possibility to ensure such duct parameters is confirmed by the results of some active experiments on the additional ionization of the background ionospheric plasma in a strong field of the antenna onboard spacecraft,[34] as well as by the theoretical study[36] of the ionization formation of a field-aligned plasma density irregularity in the near-zone field of a loop antenna.

Since we are interested in the pulsed excitation of whistler waves in the presence of a density duct, we considered the case where the frequency spectrum of the current source was concentrated in the region below the electron cyclotron frequency. In particular, we calculated the distribution of the radiated energy over the frequency spectrum for the current described by Eq. (6) with moderate values of n, and by Eq. (7) with $t_0 = \pi/2\omega_0$, assuming that the characteristic frequency ω_0 of the current in these two cases lies in the whistler range $\Omega_c < \omega < \omega_c$. It has been found that under such conditions, the dominant contribution to the radiated energy comes from the resonant part of the whistler range, i.e., the frequency interval

$$\omega_{\mathrm{LH}} < \omega < \omega_c. \tag{32}$$

Therefore, in what follows we will focus on the case where the frequency ω_0 belongs to interval (32) and analyze in detail the radiated energy going to this spectral region.

Under the above-mentioned conditions, it turns out that a single axisymmetric eigenmode, which is excited by the loop antenna with current (5) and guided by an enhanced-density duct in frequency interval (32), gives a negligible contribution to the radiated energy. This is explained by the fact at most frequencies of range (32), this eigenmode is weakly localized outside the duct[37] and, hence, has a very small excitation coefficient. As a result, the total radiated energy is approximated with high accuracy by the expression

$$W \simeq I_0^2 \int_{\omega_{\mathrm{LH}}}^{\omega_c} d\omega \int_{Q_1} w_1(q,\omega)\,dq, \tag{33}$$

where use was made of the fact that in frequency interval (32), the contribution from the $\alpha = 2$ term to the radiated energy is zero, because this term corresponds to the evanescent ordinary wave of the background magnetoplasma, i.e., wave for which $\mathrm{Re}\, h_\alpha = 0$ in this interval. Thus, the nonzero contribution of the continuous-spectrum waves to the radiated energy in the whistler range comes only from the $\alpha = 1$ term corresponding to the extraordinary, or whistler-mode wave of the background magnetoplasma. In this case, the integration region Q_1 with respect to q in Eq. (33) is semi-infinite such that $0 < q < \infty$.

To illustrate the distribution of the radiated energy over the spatial and frequency spectra, Fig. 1 shows the integrand $w_1(q, \omega)$ of Eq. (33) as a function of the integration variables q and ω in the case where $\tilde{N}/N_a = 30$ and the temporal behavior of the current is described by Eq. (6) for $n = 1$, $n = 5$, and $n = 10$ at $\omega_0 = 1.9 \times 10^5\,\mathrm{s}^{-1}$. The analogous distribution of $w_1(q, \omega)$ for a source with pulse (7) is shown in Fig. 2 for $t_0 = \pi/2\omega_0$ (the values of other parameters are the same as in Fig. 1).

It is evident from Figs. 1 and 2 that the function $w_1(q, \omega)$ for the current pulse described by Eq. (6) with $n = 1$ is qualitatively similar to that for the current given by Eq. (7) with the used value of t_0. In the figures, one can clearly see well-pronounced discrete nonoverlapping traces which correspond to sharp crests of $w_1(q, \omega)$ with respect to the q variable. The presence of such features of the distributions $w_1(q, \omega)$ on the (ω, q) plane, which makes them essentially different from the analogous functions in the case of a pulsed loop antenna in a homogeneous magnetoplasma,[33] is related to the excitation of leaky modes that are known to be guided by enhanced-density ducts in range (32).[19,37–40] The traces corresponding to the leaky modes lie above a certain boundary shown by the dashed line in each of the figures. It is also seen in Fig. 1 for the current with time dependence (6) that typical widths of localization of these traces with respect to ω tend to shrink at $\omega = \omega_0$ with increasing number n of the current half-periods that correspond to the frequency ω_0.

To clarify the position of the traces and their lower boundary in Figs. 1 and 2, we plot the normalized (to k_0) longitudinal wave number $p = h_\alpha/k_0$ as a function of q for the whistler-mode wave (at $\alpha = 1$ and $\omega < \omega_c/2$) in a homogeneous background magnetoplasma with density N_a (see the lower curve in Fig. 3). This function can be plotted using Eq. (11) and describes the refractive-index surface of the whistler-mode wave in the background magnetoplasma. In the same figure, we also present an upper curve which shows the behavior of an analogous function, but for a homogeneous magnetoplasma with density $\tilde{N}$. To plot the latter curve, one should replace the quantities ε_a, g_a, and η_a in Eq. (11) by $\tilde{\varepsilon}$, $\tilde{g}$, and $\tilde{\eta}$, respectively. In Fig. 3, the quantities $P_c = \mathcal{P}_c(N_a)$, $\tilde{P}_c = \mathcal{P}_c(\tilde{N})$, $P = (\varepsilon_a - g_a)^{1/2}$, and $\tilde{P} = (\tilde{\varepsilon} - \tilde{g})^{1/2}$ are indicated, where P and $\tilde{P}$ are the normalized propagation constants of the whistler wave traveling strictly along the external magnetic field in a homogeneous magnetoplasma with density $N = N_a$ and $N = \tilde{N}$, respectively.

In contrast to eigenmodes with the real-valued propagation constants satisfying the inequality $h_n < k_0 P_c$,[37] leaky modes supported by an enhanced-density duct have complex-valued propagation constants $h_\nu = k_0(p'_\nu - ip''_\nu)$, where ν is the radial index of such modes ($\nu = 1,2,\ldots$).[37–40] In practice, only slightly leaky modes, for which $p''_\nu \ll p'_\nu$, are of interest. Generally, the leakage is weak at the frequencies $\omega \ll \omega_c$.

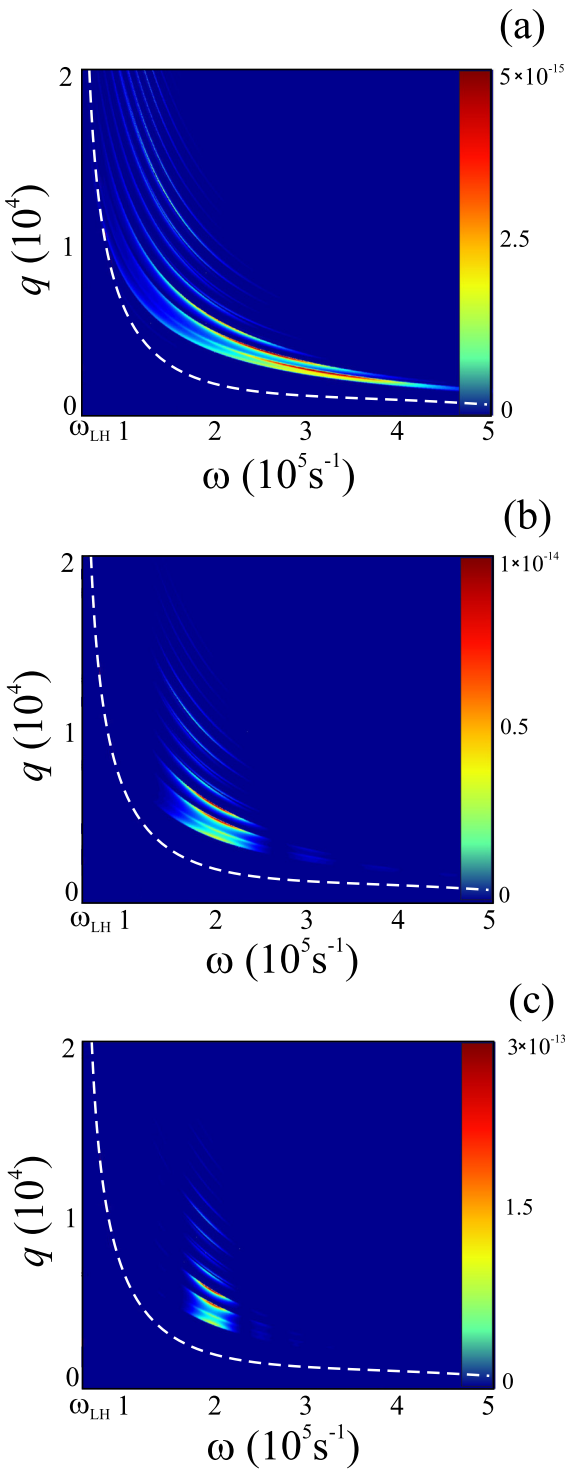

FIG. 1. Function $w_1(q, \omega)$, measured in J A^{-2} s, in the case of time dependence (6) with (a) $n = 1$, (b) $n = 5$, and (c) $n = 10$ for $\tilde{N}/N_a = 30$, $a = 5$ m, $b = 2.5$ m, $\omega_0 = 1.9 \times 10^5$ s^{-1}, $\Omega_c = 200$ s^{-1}, $\omega_c = 8.8 \times 10^6$ s^{-1}, and $\omega_{pa} = 5.6 \times 10^7$ s^{-1}. The dashed line shows the lower boundary $q = q_P(\omega)$ of the region in which slightly leaky modes exist.

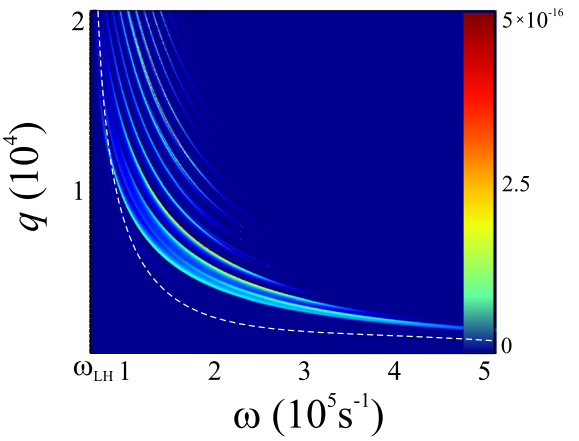

FIG. 2. The same as in Fig. 1, but for time dependence (7) with $t_0 = \pi/2\omega_0$.

These modes correspond to zeros $k_\perp = k_{\perp\nu}$ of the coefficient $C^{(2)}_{s,\alpha}$ such that $\mathrm{Im}\, k_{\perp\nu} < 0$. Therefore, the field of each slightly leaky mode outside the duct consists of the surface-type localized part, described by the second-kind Hankel function with the argument $k_{\perp\alpha}\rho$ (for which $\mathrm{Im}\, k_{\perp\alpha} < 0$ and $\alpha = 1$), and the nonlocalized part, which is described by the first-kind Hankel function with the argument $k_{\perp\nu}\rho$. The nonlocalized part corresponds to the outward-radiating wave of the quasielectrostatic type. Figure 3 shows qualitatively the mutual location of the quantities p'_ν and $q'_\nu = \mathrm{Re}(k_{\perp\nu}/k_0)$ for a leaky mode with order ν, as well as some other quantities (in particular, q_P, $q_{\min}$, and $q_{\max}$), the meaning of which is evident from the presented diagram. Recall that use of the first-kind Hankel function for the radiating part of leaky modes corresponds to the radiation condition, because the phase progress in the nonlocalized part of such modes and their outgoing energy flow are opposite in the radial direction.

Note that in the lower part of range (32) for a fixed ratio $\tilde{N}/N_a$, the inequality $P > \tilde{P}_c$ takes place, and the real parts of the propagation constants of slightly leaky modes lie in the interval $P < p'_\nu < \tilde{P}$, whence it follows that $q_P < q'_\nu < q_{\max}$. With increasing frequency ω, the quantities p'_ν start to be located in the interval $\tilde{P}_c < p'_\nu < \tilde{P}$, where $\tilde{P}_c > P$, so that

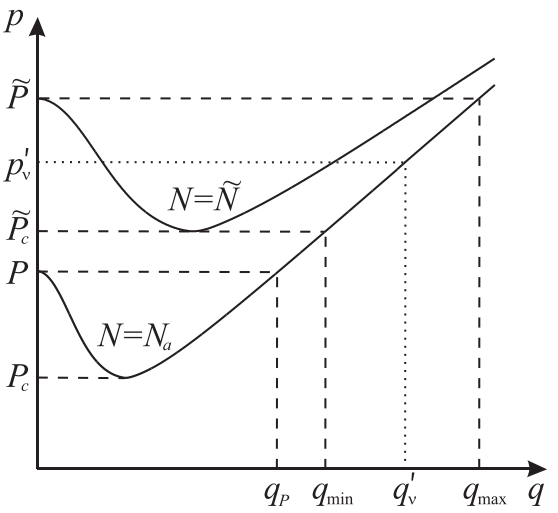

FIG. 3. Diagram explaining the features of $w_1(q,\omega)$ in the (ω,q) plane. The upper and lower solid lines correspond to the plasma densities inside and outside the duct, respectively (see text for discussion).

$q_{\min} < q'_\nu < q_{\max}$. Note that the diagram presented in Fig. 3 refers to the latter case. Since most of the radiated energy goes to slightly leaky modes with the outward-radiating parts having the dimensionless transverse wave numbers q'_ν, the positions of the brightest parts of the traces in the (ω, q) plane of Figs. 1 and 2 are given by the relationship $q = q'_\nu(\omega)$, where $q'_\nu \simeq (-\eta_a/\varepsilon_a)^{1/2} p'_\nu$. The lower boundary of these dependences, shown by the dashed line in these figures, is described by $q = q_P(\omega)$.

It is interesting to compare the distributions of the radiated energy over the spatial spectrum in Figs. 1 and 2 with the available experimental results for the field structure in the duct. It is evident that the spatial spectra of the field components are determined by the characteristic wave numbers of the most-efficiently excited leaky modes. To determine these wave numbers in the inner region of the duct for, e.g., the νth mode, we recall that its leaking part in the outer region corresponds to the outward-radiating wave with the dimensionless transverse wave number q'_ν, while the dimensionless propagation constant of this mode corresponds to the horizontal dotted line $p = p'_\nu$ in Fig. 3. This line crosses the refractive-index surface for plasma density $N = \tilde{N}$ at two points, which determine two different transverse wave numbers for the inner region. The smaller of these transverse wave numbers corresponds to an oblique whistler-mode wave, the observations of which inside the field-aligned enhanced-density irregularities were reported by many authors (see, e.g., works[13,17,22] and references therein). The greater of the above-mentioned transverse wave numbers corresponds to a small-scale quasielectrostatic whistler-mode wave in the duct. The observations of this contribution to the field in enhanced-density regions were documented in, e.g., Refs. 41–43. Note that special efforts are usually needed to reveal the presence of this small-scale part in the total field under conditions of laboratory experiments.[42,43] The neighborhoods of the above-mentioned transverse wave numbers yield predominant contributions to the spatial spectra of the field components inside the duct. Thus, although the spatial spectrum of the radiated energy does not reproduce the details of the spatial spectra of the individual field components, it allows one to correctly predict the features of the field structure in the duct.

It is obvious from Figs. 1 and 2 that integration with respect to q over each trace, which corresponds to some leaky mode, yields the individual contribution $w_\nu(\omega)$ of this mode to the normalized (to I_0^2) spectral density of the radiated energy. This means that there exists an alternative way for calculating the radiated energy in the case considered, namely,

$$W \simeq I_0^2 \int_{\omega_{\rm LH}}^{\omega_c} w_{\rm mod}(\omega)\, d\omega = I_0^2 \int_{\omega_{\rm LH}}^{\omega_c} \sum_\nu w_\nu(\omega)\, d\omega. \qquad (34)$$

It is important to note that in the whistler range, the individual contributions w_ν due to leaky modes can also be found using the technique of isolating these modes from the continuous spectrum.[15,18,19] Such a method can be more preferable, because it yields rigorous expressions for the fields of the leaky modes and their normalization quantities N_ν, which should be substituted into Eq. (28), instead of the respective quantities for eigenmodes, in order to obtain $w_\nu(\omega)$. Moreover, in the case $p''_\nu \ll p'_\nu$, the dispersion properties, field structures, excitation coefficients, and normalization quantities of whistler leaky modes as well as their contributions to the radiated energy can approximately be found using even a simpler method, according to which the leaky-mode fields outside the duct are described allowing for their localized component and neglecting the radiating quasielectrostatic component (see Refs. 16 and 19 for details). For the parameters used in this work, all the above-described methods for calculating w_ν yielded almost coinciding results. The quantities w_ν as functions of ω are shown in Fig. 4 for time dependence (6) with $n = 5$ and the previously chosen source and duct parameters. In this figure, the leaky-mode contributions w_ν to the radiated energy are shown in such a way that their projections onto the (ω, p) plane yield the dispersion curves $p = p'_\nu(\omega)$ of the leaky modes. The upper and lower red solid lines in this plane denote the boundaries $p = \tilde{P}(\omega)$ and $p = \tilde{P}_c(\omega)$, respectively, between which the real parts of the complex propagation constants of the slightly leaky modes are located for the presented frequency interval. Hereafter, the dot on the ω axis designates the frequency ω_0.

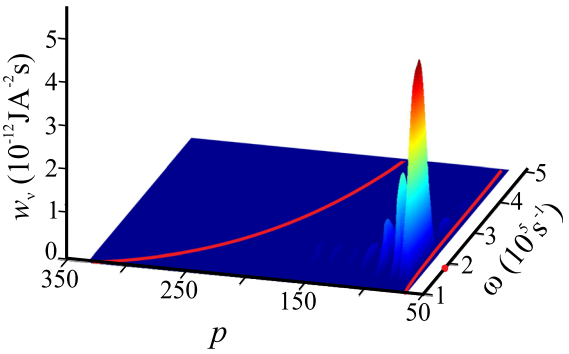

FIG. 4. Leaky-mode contributions $w_\nu(\omega)$ to the spectral density of the radiated energy for $N/N_a = 30$ and time dependence (6) with $n = 5$. The upper and lower red lines in the (ω,q) plane show the boundaries $p = \tilde{P}(\omega)$ and $p = \tilde{P}_c(\omega)$, respectively. The red dot on the ω axis designates the frequency ω_0. The source radius b, the frequency ω_0, and the duct and plasma parameters a, Ω_c, ω_c, and ω_{pa} are the same as in Fig. 1.

We now discuss the normalized spectral density $w(\omega)$ of the radiated energy. This quantity was calculated using the exact formula (27) and the approximate approach based on Eq. (34). As an example, Figs. 5–7 show the normalized distributions of the radiated energy over the frequency spectrum for a source with time dependence (6) if $n = 1$, $n = 2$ and $n = 10$, respectively. In each of these figures calculated for a duct with $\tilde{N}/N_a = 30$, the distribution corresponding to Eq. (27) is shown by the solid blue line, while the dashed red line represents the distribution $w(\omega) = w_{\rm mod}(\omega)$ corresponding to Eq. (34). It is seen in the figures that the results yielded by the two methods are qualitatively similar for a short current pulse with $n = 1$, become rather close for a longer pulse with $n = 2$, and coincide with graphical accuracy for a pulse with $n = 10$. In fact, almost perfect coincidence of the results given by the two calculation methods is already reached for $n \geq 5$. We do not present the results for time dependence (7) with $t_0 = \pi/2\omega_0$, because they are close to those shown in Fig. 5. It may be noted that a fairly good accuracy of the

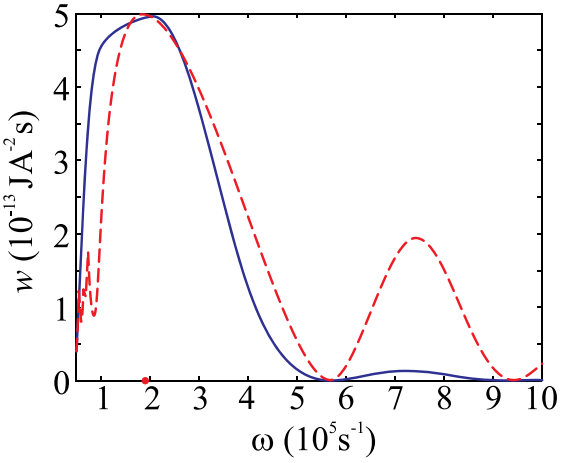

FIG. 5. Function $w(\omega)$ for time dependence (6) with $n=1$. The solid blue line and the dashed red line correspond to the exact formula and the approximation $w(\omega)=w_{\rm mod}(\omega)$, respectively. The red dot on the ω axis designates the frequency ω_0. The values of other parameters are the same as in Fig. 1.

approximation in which the individual contributions of the leaky modes to the radiated energy are added is explained by the fact that the energy orthogonality takes place with high accuracy for slightly leaky modes supported by enhanced-density ducts in the whistler range.[19]

It is important to mention that the radiated energy of the pulsed loop antenna increases with increasing plasma density inside the duct. This can be seen in Fig. 8, in which the results of calculation of $w(\omega)$ by the exact formula (27) are presented for a duct with $\tilde{N}/N_a=10$ and $\tilde{N}/N_a=30$. The rise in the radiated energy with $\tilde{N}$ is explained by an increase in the efficiency of excitation of leaky modes by a loop antenna in the whistler range with increasing plasma density in the duct.

Results of numerical calculations of the total energy radiated from the loop antenna are shown in Fig. 9 for different values of $\tilde{N}/N_a$ and the previously chosen values of a, b, ω_0, Ω_c, ω_c, and ω_{pa}. In the figure, the open circles indicate the total energy radiated from a source with time dependence (6) for various values of $n=\tau\omega_0/\pi$. The asterisks indicate the calculation results obtained using the approximate formula (34). The open squares show the energy radiated from the

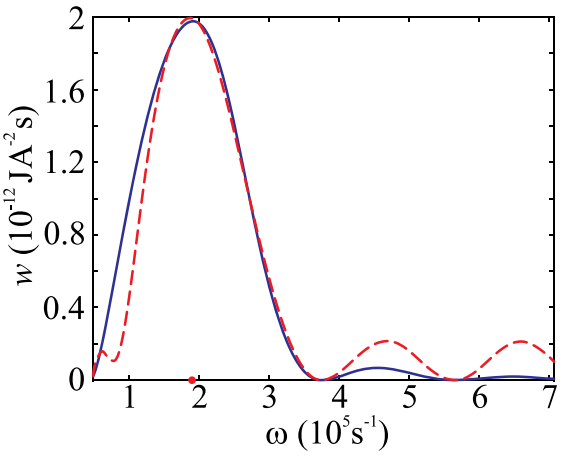

FIG. 6. The same as in Fig. 5, but for $n=2$.

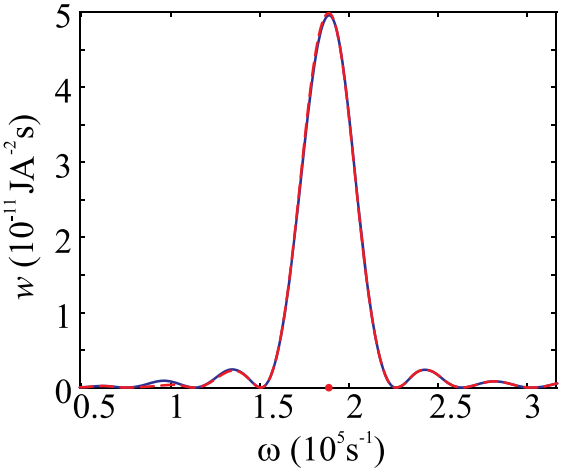

FIG. 7. The same as in Fig. 5, but for $n=10$.

source having time dependence (7) with $t_0=\pi/2\omega_0$ for the same values of ω_0 and other parameters. Note that the lower set of symbols in Fig. 9 refers to the case where the antenna is immersed in a homogeneous magnetoplasma with background density $N=N_a$. It follows from Fig. 9 that the presence of a duct with enhanced density can lead to a significant increase in the energy radiated from a pulsed loop antenna compared with the case where the same source is embedded in the surrounding homogeneous plasma medium, regardless of the current pulse duration. In addition, a fairly good accuracy of the approximate method for evaluating W on the basis of summation of the individual leaky-mode contributions is demonstrated by the obtained results. Another important implication of the numerical results is that the radiated energy in the case where the current pulse is described by Eq. (6) obeys the relation $W=\bar{P}_{\rm rad}\tau$ with good accuracy. Here, $\bar{P}_{\rm rad}$ is the time-averaged power radiated from the source possessing a time-harmonic current with the frequency ω_0. It is interesting that such behavior is observed for the current containing even a few half-periods of a monochromatic oscillation, when the parameter n is moderately small, and is related to the features of excitation of whistler

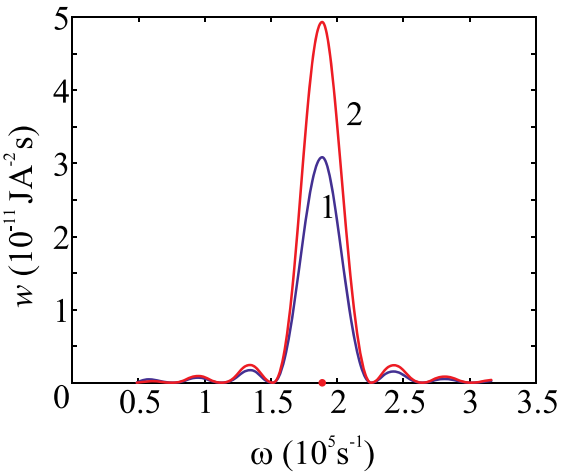

FIG. 8. Function $w(\omega)$ for a duct with $\tilde{N}/N_a=10$ (curve *1*) and $\tilde{N}/N_a=30$ (curve *2*) in the case of time dependence (6) with $n=10$. The values of other parameters are the same as in Fig. 1.

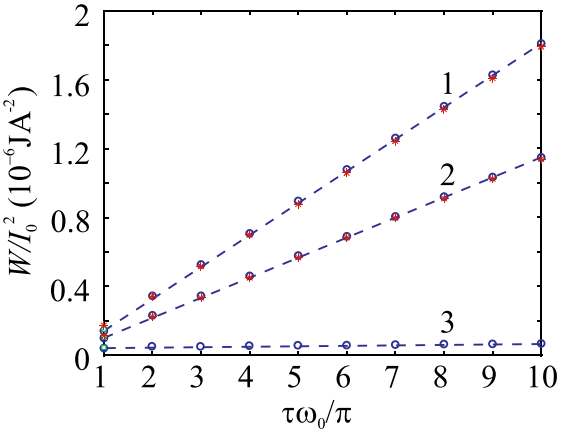

FIG. 9. Total energy radiated from a source with time dependence (6) for various values of the parameter $n = \tau\omega_0/\pi$ (circles) and from a source with time dependence (7) for $t_0 = \pi/2\omega_0$ (squares) at (*1*) $\tilde{N}/N_a = 30$, (*2*) $\tilde{N}/N_a = 10$, and (*3*) $\tilde{N}/N_a = 1$. As the characteristic duration of the latter source, the quantity $\tau = 2t_0$ is adopted. The asterisks stand for the results obtained using approximate formula (34) in the case of time dependence (6). The dashed strait lines show the energy radiated from a time-harmonic source at the frequency ω_0. The values of the parameters a, b, ω_0, Ω_c, ω_c, and ω_{pa} are the same as in Fig. 1.

leaky modes by the loop antenna immersed in an enhanced-density duct. Similar behavior of W as a function of τ in the whistler range was revealed for a pulsed loop antenna in a homogeneous magnetoplasma.[33]

It can be noted that in the case of a loop antenna located inside a sharp-walled duct, the radiated energy tends to increase with increasing antenna radius b and reaches maximum when b approaches the duct radius a. We do not present the corresponding results since the actual structure of the duct wall should necessarily be taken into account in the case $b \sim a$. However, the model of a sharp-walled duct can be used as a reasonable approximation when the loop antenna is located well inside the duct, which was assumed throughout this work. It should also be mentioned that we have neglected the ohmic loss due to collisions of charged particles in the plasma in our analysis, because the spectrum of the source current in this work is concentrated in the frequency region for which the inequality $\omega \gg \nu_e$ holds with a sufficient margin under conditions of the Earth's ionosphere (here, ν_e is the effective electron collision frequency in the plasma). Although the case where the collisional loss becomes noticeable can be considered within the framework of the developed approach, the corresponding analysis falls beyond the scope of this article.

VI. CONCLUSIONS

In this article, we have studied the whistler wave radiation from a pulsed loop antenna located in an enhanced-density duct in a magnetoplasma modeled upon the Earth's ionosphere. A notable increase in the energy radiated from this source has been found to occur in the whistler range due to the presence of such a duct. In this case, the radiated energy is predominantly determined by the discrete contributions of the slightly leaky modes which are guided by the duct and separated from the continuous part of the spatial spectrum of the excited waves. Due to this circumstance, the distribution of the radiated energy of a pulsed loop antenna over the spatial spectrum in the presence of a duct differs significantly from that of the same source immersed in an unbounded homogeneous magnetoplasma, in which case the radiated energy is relatively smoothly distributed over the spatial spectrum. It is interesting to mention that despite an increase in the radiated energy due to the presence of an enhanced-density duct, the shape of the radiated-energy distribution over the frequency spectrum, which is largely determined by the corresponding spectrum of the source current, as well as the behavior of the total radiated energy as a function of the current duration remain similar to those of the pulsed loop antenna in a homogeneous magnetoplasma.

The results of this article can be useful in explaining the data of experiments on the excitation of whistler-mode waves by pulsed sources in a magnetoplasma containing cylindrical ducts with enhanced density and planning new experiments. Future work should concentrate on an extension of the obtained results to the case of nonuniform ducts with varying parameters across and along the external magnetic field.

ACKNOWLEDGMENTS

This work was supported by the Russian Scientific Foundation (Project No. 14–12–00510). Development of some computer codes used for performing numerical calculations was supported in part by the Government of the Russian Federation (Contract Nos. 14.B25.31.0008 and 14.578.21.0033).

[1]K. G. Balmain, IEEE Trans. Antennas Propag. **12**, 605 (1964).
[2]K. G. Balmain, Radio Sci. **7**, 771, doi:10.1029/RS007i008p00771 (1972).
[3]T. N. C. Wang and T. F. Bell, Radio Sci. **4**, 167, doi:10.1029/RS004i002p00167 (1969).
[4]T. N. C. Wang and T. F. Bell, Radio Sci. **5**, 605, doi:10.1029/RS005i003p00605 (1970).
[5]T. F. Bell and T. N. C. Wang, IEEE Trans. Antennas Propag. **19**, 517 (1971).
[6]T. N. C. Wang and T. F. Bell, IEEE Trans. Antennas Propag. **20**, 394 (1972).
[7]T. N. C. Wang and T. F. Bell, J. Geophys. Res. **77**, 1174, doi:10.1029/JA077i007p01174 (1972).
[8]I. G. Kondrat'ev, A. V. Kudrin, and T. M. Zaboronkova, Radio Sci. **27**, 315, doi:10.1029/91RS02919 (1992).
[9]A. V. Karavaev, N. A. Gumerov, K. Papadopoulos, X. Shao, A. S. Sharma, W. Gekelman, A. Gigliotti, P. Pribyl, and S. Vincena, Phys. Plasmas **17**, 012102 (2010).
[10]R. L. Stenzel, Phys. Fluids **19**, 857 (1976).
[11]R. L. Stenzel, Phys. Fluids **19**, 865 (1976).
[12]H. Sugai, M. Maruyama, M. Sato, and S. Takeda, Phys. Fluids **21**, 690 (1978).
[13]G. Yu. Golubyatnikov, S. V. Yegorov, A. V. Kostrov, E. A. Mareev, and Yu. V. Chugunov, Sov. Phys. JETP **67**, 717 (1988).
[14]I. G. Kondrat'ev, A. V. Kudrin, and T. M. Zaboronkova, J. Commun. Technol. Electron. **42**, 37 (1997).
[15]I. G. Kondrat'ev, A. V. Kudrin, and T. M. Zaboronkova, Phys. Scr. **54**, 96 (1996).
[16]I. G. Kondrat'ev, A. V. Kudrin, and T. M. Zaboronkova, J. Atmos. Sol. Terr. Phys. **59**, 2475 (1997).
[17]A. V. Kostrov, A. V. Kudrin, L. E. Kurina, G. A. Luchinin, A. A. Shaykin, and T. M. Zaboronkova, Phys. Scr. **62**, 51 (2000).
[18]T. M. Zaboronkova, A. V. Kudrin, and M. Yu. Lyakh, Radiophys. Quantum Electron. **46**, 407 (2003).
[19]I. G. Kondrat'ev, A. V. Kudrin, and T. M. Zaboronkova, *Electrodynamics of Density Ducts in Magnetized Plasmas* (Gordon and Breach, Amsterdam, 1999).

[20]A. V. Kudrin, P. V. Bakharev, C. Krafft, and T. M. Zaboronkova, Phys. Plasmas **16**, 063502 (2009).
[21]W. E. Amatucci, D. D. Blackwell, D. N. Walker, G. Gatling, and G. Ganguli, IEEE Trans. Plasma Sci. **33**, 637 (2005).
[22]J. P. Pfannmöller, C. Lechte, O. Grulke, and T. Klinger, Phys. Plasmas **19**, 102113 (2012).
[23]M. V. Starodubtsev, V. V. Nazarov, and A. V. Kostrov, Phys. Rev. Lett. **98**, 195001 (2007).
[24]V. V. Nazarov, M. V. Starodubtsev, and A. V. Kostrov, Phys. Plasmas **14**, 122106 (2007).
[25]R. A. Helliwell, *Whistlers and Related Ionospheric Phenomena* (Dover, Mineola, 2006).
[26]R. L. Stenzel, J. M. Urrutia, and C. L. Rousculp, Phys. Fluids B **5**, 325 (1993).
[27]J. M. Urrutia, R. L. Stenzel, and C. L. Rousculp, Phys. Plasmas **1**, 1432 (1994).
[28]J. M. Urrutia, R. L. Stenzel, and C. L. Rousculp, Phys. Plasmas **2**, 1100 (1995).
[29]R. L. Stenzel, J. M. Urrutia, and C. L. Rousculp, Phys. Plasmas **2**, 1114 (1995).
[30]C. L. Rousculp, R. L. Stenzel, and J. M. Urrutia, Phys. Plasmas **2**, 4083 (1995).
[31]Cs. Ferencz, O. E. Ferencz, D. Hamar, and J. Lichtenberger, *Whistler Phenomena: Short Impulse Propagation* (Dordrecht, Kluwer, 2001).
[32]A. V. Streltsov, M. Gołkovski, U. S. Inan, and K. D. Papadopoulos, J. Geophys. Res. **114**, A08214, doi:10.1029/2009JA014155 (2009).
[33]A. V. Kudrin, N. M. Shmeleva, O. E. Ferencz, and T. M. Zaboronkova, Phys. Plasmas **19**, 063301 (2012).
[34]Yu. V. Chugunov and G. A. Markov, J. Atmos. Sol. Terr. Phys. **63**, 1775 (2001).
[35]V. L. Ginzburg, *The Propagation of Electromagnetic Waves in Plasmas* (Pergamon Press, Oxford, 1970).
[36]A. V. Kudrin, L. E. Kurina, and E. Yu. Petrov, JETP **92**, 969 (2001).
[37]T. M. Zaboronkova, A. V. Kudrin, M. Yu. Lyakh, and L. L. Popova, Radiophys. Quantum Electron. **45**, 764 (2002).
[38]M. J. Laird and D. Nunn, Planet. Space Sci. **23**, 1649 (1975).
[39]V. I. Karpman and R. N. Kaufman, J. Plasma Phys. **27**, 225 (1982).
[40]T. M. Zaboronkova, A. V. Kudrin, and G. A. Markov, Plasma Phys. Rep. **19**, 397 (1993).
[41]I. A. Vdovichenko, G. A. Markov, V. A. Mironov, and A. M. Sergeev, JETP Lett. **44**, 275 (1986).
[42]D. D. Blackwell, T. G. Madziwa, D. Arnush, and F. F. Chen, Phys. Rev. Lett. **88**, 145002 (2002).
[43]J. F. Bamber, W. Gekelman, and J. E. Maggs, Phys. Rev. Lett. **73**, 2990 (1994).